Evaluation of flow resistance in smooth rectangular open channels with modified Prandtl friction law

Cheng, Nian-Sheng; Nguyen, Hoai Thanh; Zhao, Kuifeng; Tang, Xiaonan

2011

Cheng, N. S., Nguyen, H. T., Zhao, K., & Tang, X. (2011). Evaluation of Flow Resistance in Smooth Rectangular Open Channels with Modified Prandtl Friction Law. Journal of Hydraulic Engineering, 137(4), 441-450.

https://hdl.handle.net/10356/101741

https://doi.org/10.1061/(ASCE)HY.1943-7900.0000322

Evaluation of flow resistance in smooth rectangular open-channels with modified Prandtl friction law

Nian-Sheng Cheng[1], Hoai Thanh Nguyen[2], Kuifeng Zhao[3], and Xiaonan Tang[4]

[1]Associate Professor, School of Civil and Environmental Engineering, Nanyang Technological University, Nanyang Avenue, Singapore 639798. Email: cnscheng@ntu.edu.sg

[2]Research Student, School of Civil and Environmental Engineering, Nanyang Technological University, Nanyang Avenue, Singapore 639798.

[3]Project Officer, DHI-NTU Water & Environment Research Centre and Education Hub, Nanyang Technological University, Nanyang Avenue, Singapore 639798.

[4]Research Fellow, The University of Birmingham, Edgbaston, Birmingham, B15 2TT, UK. E-mail: x.tang@bham.ac.uk

Abstract

Flow resistance in open channels is usually estimated by applying the approach that is developed originally for pipe flows. Such estimates may be useful for engineering applications, but they always differ to some extent from measurements. This paper first summarizes empirical approaches that have been proposed in the literature to reconcile the resistance difference, which include various modifications of the pipe friction for applications to rectangular ducts and open channel flows. An improved friction equation is then derived for evaluating flow resistance of smooth rectangular open channels.

Comparisons are made with experimental data reported by previous researchers and those collected in the present study. It is shown that the new proposed equation is applicable for both narrow and wide channels and more accurate than those available in the literature.

Keywords: open channel, resistance, pipe friction

Introduction

Many studies of flow resistance in open channels have been conducted in the past decades, of which a complete review would be in itself a challenging task (Yen 2002). However, no general method is available for dealing with data obtained even with smooth rectangular channels of different width-to-depth or aspect ratios. This is largely due to the existence of the non-uniform distribution of boundary shear stress and free surface, which causes open channel flows more complicated than circular pipe flows. On the other hand, for practical applications, open channel friction could be directly estimated by applying the approach developed originally for pipe flows. It should be noted that the channel friction so obtained generally deviates from measurements; therefore various modified equations based on the standard flow friction of pipes have been proposed for open channel flows.

The present study first reviews various empirical approaches that have been proposed in the literature to reconcile the flow resistance difference between circular pipes and rectangular channels, which consist of various modifications of the pipe friction equation. An improved friction equation is then derived for evaluating rectangular open channel friction for the case of smooth boundary. Comparisons are made with experimental data reported by previous researchers and also those collected in the present study. Finally, it is shown that the present equation is applicable for a wide range of aspect ratios and more accurate than those available in the literature.

Modifications of Prandtl's friction law for open channel flows

Since Nikuradse performed the celebrated experiments in the 1930s, the dependence of the pipe friction factor on the Reynolds number has been well understood for both smooth and rough pipes (Nikuradse 1933, Schlichting 1979). The dependence can be analytically formulated using the logarithmic law to approximate the velocity profile over the entire cross section of the flow. For example, the resulting formula for smooth pipe flows, which is usually referred to as Prandtl's friction law, is expressed as

$$\frac{1}{\sqrt{f}} = c_{10} \log(\mathrm{Re}\sqrt{f}) - c_{20} \tag{1}$$

where f is the friction factor, Re = VD/ν, V is the average velocity, D is the pipe diameter, ν is the kinematic viscosity of fluid, and c_{10} and c_{20} are the constants. With Nikuradse's experimental data, Prandtl obtained $c_{10} = 2$ and $c_{20} = 0.8$ (Schlichting 1979).

Eq. (1) has also been applied to other wall-bounded flows such as non-circular pipes and open channel flows. It is noted that such extensions are useful for practical applications, although the friction factors so estimated always differ to some extent from measurements. For example, Myers (1982) reported that on average, the channel friction factor was greater than the equivalent pipe value by 8.3%. After reviewing historical data of turbulent friction in smooth rectangular ducts, Jones (1976) concluded that the non-circular duct friction scatters around the Prandtl's friction law by approximately -5 to 15%. Knight's (1984) measurements show that smooth channel friction factors are 5 to 10% higher than those predicted by the Prandtl equation. Moreover, the discrepancies reported cannot be simply interpreted in terms of surface roughness or inadequate development of the flow field (Jones 1976, Knight 1984).

To classify various approaches proposed in the previous studies, the Prandtl's friction law is rewritten in the form

$$\frac{1}{\sqrt{f_E}} = c_1 \log(\mathrm{Re}_E \sqrt{f_E}) - c_2 \qquad (2)$$

where $f_E = m_f f_{ch}$, $\mathrm{Re}_E = m_{Re}\mathrm{Re}_{ch}$, f_E is the equivalent friction factor, Re_E is the equivalent Reynolds number, f_{ch} (= $8gR_hS/V^2$) is the open channel friction factor, Re_{ch} (= $4R_hV/\nu$) is the open channel Reynolds number, R_h is the hydraulic radius, S is the energy slope, m_f and m_{Re} are the modification coefficients, and c_1 and c_2 are the modified constants.

With Eq. (2), all the previous approaches can be then categorized into (1) Modification of the two constants, taking $m_f = m_{Re} = 1$; (2) Modification of the friction factor, taking $c_1 = c_{10}$, $c_2 = c_{20}$, $m_{Re} = 1$ and $f_E = m_f f_{ch}$; and (3) Modification of the Reynolds number, taking $c_1 = c_{10}$, $c_2 = c_{20}$, $\mathrm{Re}_E = m_{Re}\mathrm{Re}_{ch}$ and $m_f = 1$. Further discussions on these modifications are followed next.

(1) Modification of the two constants

Keulegan (1938) pioneered the study of open channel friction by developing analytical formulas in the form similar to that obtained by Nikuradse for circular pipes. He stated that the two constants, c_{10} and c_{20}, depend on the characteristics of the wall-confined turbulence and the channel surface finish, respectively.

Keulegan's analysis includes two assumptions. The first is that the logarithmic velocity distribution is generally applicable near a solid boundary. The second is related to combined effects of secondary currents and free surface, which were considered to be a small quantity being merged in c_2. The resulting friction formula for open channels is then identical in form to that for circular pipes, but with different constants. The analysis presented by Keulegan, though incomplete in fixing the constants, has been followed by many subsequent researchers. However, it should be noted that the experimental data used in Keulegan's analysis are limited to those collected by Bazin in the years 1855 to 1860.

Empirically, the adjustment of the two constants (c_1, c_2) can also be visualized by plotting experimental data of f_{ch} and Re_{ch} in the form of $1/\sqrt{f_{ch}}$ against $Re_{ch}\sqrt{f_{ch}}$. The plot so obtained usually shows that the channel friction deviates almost consistently from the Prandtl's friction law for smooth boundary conditions (e.g., see Fig. 1). Therefore, empirical adjustment of the two constants is a simple way to roughly estimate the friction for channels with non-circular cross sections. Table 1 summarizes various values of c_1 and c_2 being reported in the literature. It can be seen that c_1, the slope of the data trend in Fig. 1, varies in a limited range (from 1.81 to 2.14), while c_2, the intercept, varies widely from 0.35 to 1.83.

(2) Modification of the friction factor

Kazemipour and Apelt (1979) suggested that the friction factor for channels with non-circular cross sections be corrected as $\psi_{KA}f_{CW}$, where ψ_{KA} is the shape factor and f_{CW} was computed using the Colebrook-White formula at given Reynolds numbers. By noting that the Colebrook-White equation reduces to the Prandtl's friction law for smooth pipes, and comparing the suggested corrections in Eq. (2), it is obtained that $m_f = 1/\psi_{KA}$ and $m_{Re} = 1$.

Kazemipour and Apelt further defined the shape factor as $\psi_{KA} = \psi_1/\psi_2$, where ψ_1 and ψ_2 were used to account for non-uniform distribution of boundary shear stress and effect of aspect ratio, respectively. For rectangular open channels, $\psi_1 = \sqrt{(\alpha+2)/\alpha}$, where α = B/h, B is the channel width and h is the flow depth. The dependence of ψ_2 on α was presented as a curve by Kazemipour and Apelt, which was calibrated using the experimental data collected by Tracy and Lester (1961) and Shih and Grigg (1967) for smooth rectangular open-channels. For convenience, the Kazemipour and Apelt's curve is represented in the present study by the following formula (see Fig. 2),

$$\psi_2 = \frac{1}{1.09 - 1.13\exp(-0.82\sqrt{\alpha})} \quad (3)$$

Therefore,

$$m_f = \frac{1}{1.09 - 1.13\exp(-0.82\sqrt{\alpha})}\sqrt{\frac{\alpha}{2+\alpha}} \quad (4)$$

In spite of the fact that the ψ_2-α relationship was developed using the data only for smooth rectangular open channels, Kazemipour and Apelt further showed that their approach was also applicable for rough rectangular channels and smooth channels of triangular and trapezoidal sections.

Pillai (1997) considered m_f as a function of P/R_h [$=(2+\alpha)^2/\alpha$], where P is the wetted perimeter and R_h is the hydraulic radius, and obtained the following empirical relationship:

$$m_f = 0.898 + 0.034\mathrm{e}^{0.195(10-s)} \quad (5)$$

where

$$s = \begin{cases} (2+\alpha)^2/\alpha & \text{for} \quad \alpha \geq 2 \\ 16-(2+\alpha)^2/\alpha & \text{for} \quad 0.656 \leq \alpha \leq 2 \\ (2+\alpha)^2/\alpha - 5.5 & \text{for} \quad \alpha < 0.656 \end{cases} \quad (6)$$

Pillai's analysis was performed based on the same data used by Kazemipour and Apelt (1979). Comparisons between Eq. (5) and Eq. (4) in Fig. 3 show that they are close only when $3 < \alpha < 40$.

(3) Modification of the Reynolds number

Jones (1976) noted that the low aspect ratio data in general tend to agree with the prediction using the Prandtl's friction law, while the high aspect ratio data are greater than the prediction. By comparing the Prandtl equation with turbulent flow data of smooth rectangular ducts , Jones (1976) concluded that the hydraulic diameter is not the proper length dimension to use for the Reynolds number to ensure similarity between circular and rectangular ducts. By exploring the different friction relations derived for circular pipes and non-circular ducts, Jones defined a 'laminar equivalent' diameter to modify the Reynolds number. With the modified Reynolds number, Jones was able to reduce the error in the prediction of channel friction from a scatter band of -5 to 20% to $\pm$5%.

For rectangular ducts, Jones proposed that

$$m_{\mathrm{Re}} = \frac{2}{3}\left(1+\frac{1}{A_r}\right)^2 \left[1-\frac{192}{\pi^5 A_r}\sum_{n=0}^{\infty}\frac{1}{(2n+1)^5}\tanh\frac{(2n+1)\pi A_r}{2}\right] \tag{7}$$

where A_r is the aspect ratio of duct. In spite of the free surface effect, a rectangular open channel is comparable to half of a rectangular duct, as demonstrated by Knight (1984) through experimental observations of the boundary shear stress distribution. By noting that $A_r = \alpha/2$, Eq. (7) can be then applied for open channels in the revised form,

$$m_{\mathrm{Re}} = \frac{2}{3}\left(1+\frac{2}{\alpha}\right)^2 \left[1-\frac{384}{\pi^5 \alpha}\sum_{n=0}^{\infty}\frac{1}{(2n+1)^5}\tanh\frac{(2n+1)\pi \alpha}{4}\right] \tag{8}$$

Obot (1988) attempted to associate the friction variation from circular to non-circular channels with flow transition phenomena, and then scaled the Reynolds number and friction factor of non-circular channels with their respective critical values. By noting that the friction factor at transition remains almost constant for circular, rectangular and triangular cross-sections, the Reynolds number is the only variable to be modified to reconcile friction differences between circular and non-circular cross-sections. Therefore

Obot defined a scale factor, ψ_{OB}, to reduce the Reynolds number in the form of $\psi_{OB}Re_{ch}$ = Re_E, which implies that $m_{Re} = \psi_{OB}$. The experimental data summarized by Obot show that ψ_{OB} varies with the aspect ratio, A_r, for rectangular ducts. The relation between m_{Re} and A_r, as plotted in Fig. 4, can be approximated as

$$\psi_{OB} = \frac{1}{3}\left(2 + e^{-0.06A_r}\right) \tag{9}$$

When applied to open channel flows, Eq. (9) is rewritten as

$$m_{\mathrm{Re}} = \frac{1}{3}\left(2 + e^{-0.03\alpha}\right) \tag{10}$$

Obot reported that the pipe friction equation remains if the reduced Reynolds number is used for non-circular cross-sections and application of ψ_{OB} is comparable to the use of 'laminar equivalent' diameter proposed by Jones (1976). However, the comparison of Eqs. (7) and (9) shows that the difference between the two approaches is obvious, as seen in Fig. 4.

Present consideration

First, consider smooth rectangular channels of $B \geq 2h$ or $\alpha \geq 2$. In light of the approach developed by Keulegan (1938), the half cross section is divided into two zones, i.e. the corner zone ($x < h$) and the central zone ($h < x < 0.5B$), as sketched in Fig. 5(a). It should be noted that this division seems artificial and does not represent exactly complicated structures of open channel flows, the latter being not well understood at present (Yang and Lim 1997). However, it facilitates mathematical treatment for the rational determination of the cross-section average velocity in open channels, as demonstrated subsequently. A further discussion on the division approach is given later in this paper.

In the corner zone, the corner bisector is used to further divide the area into two parts: the lower part being affected by the channel bed and the upper part by the side wall. It is known both secondary flow and free surface effects could affect the velocity profile, particularly in the zone near the wall, but there is no general formula to describe such a profile at present. However in a close examination of 3D flow structure, Yang and Lim (1997) have found that the log law can be used to express the velocity distribution near the bed. By considering the continuity of flow in the corner secondary flows, it is assumed that the contributions of the two parts of the corner zone to the average velocity are approximately the same. Similar to the analysis by Adachi (1962), the velocity profiles are generally approximated using the logarithmic law,

$$\frac{u}{u_*} = \frac{1}{\kappa} \ln\left(A \frac{u_* y}{\nu} \right) \tag{11}$$

where y is the vertical distance from the channel bed, u_* is the local shear velocity, κ is the von Karman constant and A is a constant. Because of the existence of sidewalls and secondary flows, the bed shear stress and thus the shear velocity vary laterally. Knight's (1984) data show that the shear stress declines slowly towards the sidewall from its peak value, which occurs almost at the middle of the channel. It appears that the measured reduction can be approximated using a power function, e.g.

$$\frac{\tau_b}{\tau_{b\max}} = \left(\frac{x}{0.5B} \right)^{2m} \qquad \text{or} \qquad \frac{\tau_b}{\tau_{bmean}} = (2m+1)\left(\frac{x}{0.5B} \right)^{2m} \tag{12}$$

and therefore,

$$\frac{u_*}{u_{*\max}} = \left(\frac{x}{0.5B} \right)^{m} \tag{13}$$

where x is measured laterally from the sidewall, and m is a constant. Knight's (1984) shear stress data suggest that $m \approx 0.045$, as shown in Fig. 6.

With the above considerations, the sectional average velocity for B $\geq$ 2h can be computed by

$$V = \frac{1}{Bh}\left(2\int_0^h\int_0^x u\,dy\,dx + \int_h^{0.5B}\int_0^h u\,dy\,dx\right) \tag{14}$$

Substituting Eqs. (11) and (13) into Eq. (14) gives

$$\frac{V}{u_{*mean}} = \frac{\lambda}{\kappa}\left[a_1 \ln\left(\frac{1+w}{w}\frac{\lambda A}{4}\mathrm{Re}\frac{u_{*mean}}{V}\right) - a_2\right] \tag{15}$$

where Re = $4R_hV/\nu$ is the hydraulic diameter based Reynolds number, R_h (= Bh/(B+2h)) is the hydraulic radius, w = B/(2h) = α/2, and λ, a_1 and a_2 are the coefficients given as follows,

$$\lambda = \frac{u_{*\max}}{u_{*mean}} = \sqrt{\frac{(2m+1)(w+1)}{w+w^{-2m}}} \tag{16}$$

$$a_1 = \frac{1}{m+1} + \frac{m}{(m+2)(m+1)w^{m+1}} \tag{17}$$

$$a_2 = \frac{m^2\ln(w)}{(m+2)(m+1)w^{m+1}} + \frac{2m^3+5m^2+4m+2}{(m+2)^2(m+1)^2w^{m+1}} + \frac{2m+1}{(m+1)^2} \tag{18}$$

Bearing in mind, Eq. (14) is derived using a logarithmic law to approximate the velocity profile, which might not be accurate in the regions near the wall due to effects of secondary flows and free-surface; however it is considered relatively appropriate by noting uncertainties in the other parameters and data used, as discussed subsequently. Alternatively, possible deviations of the prediction can be taken into account by merging them into the three parameters, i.e. *m*, κ and A, which are to be calibrated with data. Such ideas were developed previously by Prandtl (Schlichting 1979) and Keulegan (1938). Therefore, it is expected that the performance of Eq. (15) can be improved further using the parameters with optimized values. To this end, a series of computations were conducted by taking *m* = 0 – 0.2, κ = 0.35 – 0.45, and A = 5 – 15, with the data by Tracy and Lester (1961) who measured the channel friction for both subcritical and supercritical flows with α = 6.96 - 40.37. The computed results were then used to observe prediction error variations with the three parameters.

Fig. 7(a) shows the variation of the prediction error with κ for A = 9 and m = 0 – 0.2. For each m, the error first reduces with increasing κ, until it reaches a minimum at a critical κ-value, and afterwards, the error increases again with κ. Furthermore, as m changes gradually from 0 to 0.2, the minimum error slightly increases and the related critical κ-value varies from 0.42 to 0.435. Fig. 7(b) shows similar variations of the prediction error with A for κ = 0.42 and m = 0 – 0.2. It shows that the minimum error decreases slowly as m changes from 0.2 to 0, and the best prediction occurs at about A = 9.

Fig. 8 further presents the variation range of the prediction error, which minimizes at $m \approx 0$, $\kappa \approx 0.42$ and A $\approx$ 9. It is interesting to note that (1) there are only slight changes in both m and κ to achieve the best performance of the derived formula; (2) the m-value reduces to 0 from 0.045, the latter being estimated using Knight's data; and (3) the κ-value obtained differs from the traditionally recommended 0.40, but is very close to 0.422 derived from the recently-published pipe flow data (McKeon et al. 2005).

Simplification of the present approach

With the above sensitive analysis on the parameters, the approach proposed in this study can be further simplified. By substituting $m \approx 0$ into Eqs. (16) to (18), it follows that λ = 1, a_1 = 1 and a_2 = 1 + 1/(2w). Eq. (15) is then rewritten as

$$\frac{V}{u_{*mean}} = \frac{1}{\kappa}\left[\ln\left(\frac{1+w}{w}\frac{A}{4}\mathrm{Re}_{ch}\frac{u_{*mean}}{V}\right) - \left(1+\frac{1}{2w}\right)\right] \tag{19}$$

or in the form of Eq. (1),

$$\sqrt{\frac{1}{m_f f_{ch}}} = 2\log\left(m_{\mathrm{Re}}\mathrm{Re}_{ch}\sqrt{m_f f_{ch}}\right) - 0.8 \tag{20}$$

where

$$m_f = \left(2\sqrt{8}\,\kappa\log(e)\right)^{-2} \approx 0.939, \tag{21}$$

$$m_{Re} = \frac{2.51A\kappa\log(e)}{2}e^{-1-\frac{1}{2w}}\frac{1+w}{w} \approx 0.758\frac{1+w}{w}e^{-\frac{1}{2w}} \tag{22}$$

and $f_{ch} = 8\left(u_{*mean}/V\right)^2$. To avoid iterative procedure of computing f_{ch} in Eq. (20), by following the approximation proposed by Haaland (1983), Eq (20) can be expressed as

$$f_{ch} = \left[1.8\sqrt{m_f}\log\left(\frac{m_{\mathrm{Re}}\mathrm{Re}_{ch}}{6.9}\right)\right]^{-2} \approx 0.33\left[\log\left(0.11\mathrm{Re}\frac{1+w}{w}e^{-\frac{1}{2w}}\right)\right]^{-2} \tag{23}$$

It should be noted that the limitation of $B \geq 2h$ or $\alpha \geq 2$ is applied in deriving Eqs. (15) and (20). However, for narrow channel flows in the case of $B < 2h$ or $\alpha < 2$, the two equations in exactly the same form can also be derived by applying the corner division approach (see Fig. 5(b)) and the logarithmic velocity distribution to the half cross section, provided that w is revised to be $2h/B$ or $2/\alpha$. Therefore, Eqs. (15), (20) or (23) applies for both narrow and wide channel flows with *w* expressed in the following general form,

$$w = \begin{cases} \alpha/2 & if \quad \alpha \geq 2 \\ 2/\alpha & if \quad \alpha < 2 \end{cases} \qquad \text{or} \qquad w \approx \left[\left(\frac{\alpha}{2}\right)^k + \left(\frac{2}{\alpha}\right)^k\right]^{1/k} \tag{24}$$

where $k \approx 10$.

Experiments

To compare the flow resistance formulae of the present approach (i.e. Eq. (20) or (23)) with the previous modifications, experiments were also conducted in this study using three different sizes of tilting flumes under various uniform flow conditions. The width (m) x length (m) of the flumes were 0.075 x 5, 0.30 x 12, and 0.60 x 14, respectively. The data collected are summarized in Table 2. The aspect ratio (α = B/h) varied from 1.07 to 15, Reynolds number (Re = $4R_hV/\nu$) from 7.7 x 10^3 to 5.4 x 10^5, and Froude number (Fr = $V/\sqrt{gh}$) from 0.24 to 0.75. Flow discharges were measured as an average of more than 100 readings taken from a built-in turbine or electromagnetic flowmeter, which was verified regularly using a portable ultrasonic flow meter. The flowmeter reading varied and its standard deviation was about 0.2-1.3%. The channel slopes were calculated from longitudinal flow depth variations, which were measured using a point gauge accurate to 0.1 mm while water in the flume remained stationary. Extra care was taken in measuring the short flume slope. Each case of uniform flow was achieved by a process of trial and error. For a given bed slope, the applied flow rate was estimated using the Manning equation by taking n = 0.01, and the flow depths were then measured at five preselected sections in the working region of the flume. Both the tailgate and pump speed were then adjusted repeatedly until the measured flow depths were almost the same at the five sections. Large fluctuations occurred in the measurement of flow depth for cases of large bed slope and high flow velocity. The kinematic viscosity of water, ν (in m^2/s), was calculated by the formula proposed here,

$$\nu = \left(\frac{60}{T+40} \right)^{1.45} 10^{-6} \tag{25}$$

where T is the temperature in degree Celsius. Eq. (25) applies for T = 0 - 100°C, and agrees with the standard dataset given by Linstrom and Mallard (2005), with errors less than 0.54% for T = 0-100°C.

Comparisons of different approaches

The general procedure for computing the open channel friction factor is given as follows:

(1) First, work out the two modification coefficients, m_{Re} and m_f;

(2) Then, calculate Re_E (= $m_{Re}Re_{ch}$), and substitute it into the Prandtl's friction law or Eq. (2) to get f_E; and

(3) Finally, f_{ch} is calculated to be f_E/m_f.

Plotted in Fig. 9 is an example of the variations of the predicted friction factor with the aspect ratio at Re = 10^6 using the different formulas proposed previously and in the present study. It can be seen that for high aspect ratios (α > 8), the present approach predicts similar results to those given by Kazemipour and Apelt (1979) and Pillai (1997), while for very narrow channels (α < 0.2), the present prediction is comparable only to that given by Pillai (1997). The methods that were proposed for rectangular ducts by Jones (1976) and Obot (1988), respectively, generally underestimate the open channel friction. This observation is also confirmed in Fig. 10. In addition, it is interesting to note that the friction factor predicted using Eq. (23) varies in the way similar to that given by Jones' (1976) approach, the latter being developed based on the concept of 'laminar-equivalent diameter". It should be mentioned that the variations shown in Fig. 9 are computed for α = 0.1 – 100, which is much wider than the range of the experimental data used subsequently (see Table 3).

Fig. 10 shows comparisons of the predicted and measured friction factor for α = 0.3 – 40.4 and Re = $7.7 \times 10^3 - 7.3 \times 10^5$ (see Table 3). The data used were presented previously by Tracy and Lester (1961) and Knight (1984), in addition to those collected in this study. The difference between prediction and measurement is assessed using the error defined by

$$error = \frac{|prediction - measurement|}{measurement} \times 100\,(\%) \qquad (26)$$

The average and maximum errors obtained using the different methods are summarized in Table 4. By applying the original Prandtl's friction law with no modifications, the predicted channel friction gives an average error of 9.1%, and could underestimate by up to 20.4%. This prediction is improved by the four empirical methods reviewed in the present study. However, the predicted channel friction is generally underestimated, in particular, by the methods developed by Jones (1976) and Obot (1988), respectively. The other two methods, proposed by Kazemipour and Apelt (1979) and Pillai (1997), respectively, predict friction factors with similar accuracies, as expected because they were developed from the same database. Among the four approaches, Pillai's method is the only one applicable to narrow channels, and thus performs better in terms of overall average error. By comparing with all the empirical approaches, the analytical equation (20 or 23) proposed in this study provides the best friction prediction for both narrow and wide smooth rectangular channels, with the average error reduced to 2.1% and 3.5% for $B > 2h$ and $B \leq 2h$, respectively. Fig. 11 shows the distribution of errors in the prediction of friction factor using Eq. (23).

Discussion

In open channel flows, effects of free surface and secondary currents may not be negligible. However, how to quantify such effects into the evaluation of flow resistance is still a challenging task. For example, the log-wake law may be applicable to delineate the free-surface effect on flow velocity profiles. However, there is not such a wake function that is available in a general form. On the other hand, it has been observed that secondary currents appear considerably weak, in comparison to the longitudinal or primary flows in open channels. For example, Montes (1998) noted that the velocity of secondary currents is two orders of magnitude smaller than or about 1-2% of the main flow velocity. Wang and Cheng (2006) observed that the maximum vertical velocity was only 0.6-2.5% of the depth-averaged velocity for the secondary currents that were induced by the lateral variation of the bed roughness in a wide channel. In addition, the production of secondary currents could be well explained by considering gradients of Reynolds stresses (Montes 1998). Therefore, the effect of secondary currents on the primary flow could be effectively evaluated using highly complex models, which is beyond the objective of the present study.

However, in spite of complex 3D flows, there is a general agreement that flows in a simple rectangular channel can be analyzed in the central zone with 2D features and near wall zones with strong secondary flows, as demonstrated, for example, by Tracy and Lester (1961). In the corner zone, Keulegan (1938) proposed a simple straight line to divide the corner zone into two, one corresponding to the bed and the other to the sidewalls. The rationality of the simplification has been confirmed by subsequent researchers, for example, De Cacqueray et al (2009), who have recently demonstrated that an approximate zero stress division line exists along the bisector for a smooth rectangular channel when $B/h > 2$ using a high order Reynolds stress model.

Despite some approximations made in the derivation of the flow resistance equation, Eq. (15), as discussed above, it is appropriate to apply the resulting Eq. (19) or (23) to evaluation of the flow resistance as the three parameters, i.e. m, κ and A, were evaluated through a large set of experimental data. However, it should be noted that Eq. (19) or (23) could be improved when more data are available.

Conclusions

With the concept of hydraulic diameter, the Prandtl's pipe friction law can be used to predict the open channel friction, which could lead to a deviation of up to 20% from measurement. In the present study, various approaches available in the literature are first unified, which apply empirical modifications to either Reynolds number, friction factor, or the constants involved in the Prandtl's friction law. Then, the log law is used to approximate the velocity profile over the cross section and a new analytical approach is thus derived for the evaluation of the flow resistance in smooth rectangular channels. The results show that both friction factor and Reynolds number need to be modified in the application of the Prandtl's friction law to open channel flows. In comparison with all the empirical approaches, the new analytical equation applies for both narrow and wide channels and provides the best friction prediction for smooth rectangular channels. However, it should be mentioned that the comparisons were made based on the limited data, of which the aspect ratio varied from 0.3 to 40.4 and the Reynolds number from 7.7×10^3 to 7.3×10^5.

References

Adachi, S., (1962). "The effect of side walls in rectangular cross sectional channel." *Transactions of the ASCE*, 82, 17-26.

De Cacqueray, N., Hargreaves, D. M., and Morvan, H. P., (2009). "A computational study of shear stress in smooth rectangular channels." *Journal of Hydraulic Research*, 47 (1), 50-57.

Haaland, S. E., (1983). "Simple and explicit formulas for the friction factor in turbulent pipe-flow." *Journal of Fluids Engineering-Transactions of the ASME*, 105 (1), 89-90.

Jones, O. C. J., (1976). "An improvement in the calculation of turbulent friction in rectangular ducts." *Journal of Fluids Engineering*, 98, 173-180.

Kazemipour, A. K. and Apelt, C. J., (1979). "Shape effects on resistance to uniform flow in open channels." *Journal of Hydraulic Research*, 17 (2), 129-147.

Keulegan, G. H., (1938). "Laws of turbulent flow in open channels." *Journal of Research of the National Bureau of Standards*, 21, 707-741.

Knight, D. W., (1984). "Boundary shear in smooth rectangular channels." *Journal of Hydraulic Engineering, ASCE*, 110 (4), 405-422.

Linstrom, P. J. and Mallard, W. G., (2005). *Thermophysical properties of fluid systems*. NIST standard reference database No. 69. National Institute of Standards and Technology, http://webbook.nist.gov, Gaithersburg MD.

McKeon, B. J., Zagarola, M. V., and Smits, A. J., (2005). "A new friction factor relationship for fully developed pipe flow." *Journal of Fluid Mechanics*, 538, 429-443.

Montes, S., (1998). *Hydraulics of open channel flow*. ASCE Press, Reston, VA.

Myers, W. R. C., (1982). "Flow resistance in wide rectangular channels." *Journal of Hydraulic Division, ASCE*, 108 (4), 471-482.

Nikuradse, J., (1933). "Stromungsgesetze in rauhen Rohren." *Forschung auf dem Gebiete des Ingenieurwesens*, Forschungsheft 361. VDI Verlag, Berlin, Germany (in German). (English translation: Laws of flow in rough pipes, NACA TM 1292, 1950).

Obot, N. T., (1988). "Detremination of incompressible flow friction in smooth circular and noncircular passages: A general approach including validation of the nearly century old hydraulic diameter concept." *Journal of Fluids Engineering*, 110, 431-440.

Pillai, N. N., (1997). "Effect of shape on uniform flow through smooth rectangular open channels." *Journal of Hydraulic Engineering*, 123 (7), 656-658.

Schlichting, H., (1979). *Boundary-layer theory*. 7th ed. McGraw-Hill series in mechanical engineering. McGraw-Hill, New York.

Shih, C. C. and Grigg, N. S., (1967). "A reconsideration of the hydraulic radius as a geometric quanity in open channel hydraulics." *Proceedings of 12th Congress, IAHR*. 288-296.

Tracy, H. J. and Lester, C. M., (1961). "Resistance coefficients and velocity distribution, smooth rectangular channel." *Geological Survey Water-Supply Paper No. 1592-A*.

Wang, Z. Q. and Cheng, N. S., (2006). "Time-mean structure of secondary flows in open channel with longitudinal bedforms." *Advances in Water Resources*, 29 (11), 1634-1649.

Yang, S. Q. and Lim, S. Y., (1997). "Mechanism of energy transportation and turbulent flow in a 3D channel." *Journal of Hydraulic Engineering-ASCE*, 123 (8), 684-692.

Yen, B. C., (2002). "Open channel flow resistance." *Journal of Hydraulic Engineering-ASCE*, 128 (1), 20-39.

Notation

The following symbols are used in this paper:

A	constant
A_r	aspect ratio of duct
a_1, a_2	coefficient
B	channel width
c_1, c_2, c_{10}, c_{20}	constant
D	pipe diameter
Fr	Froude number (= $V/\sqrt{gh}$)
f	friction factor
f_{ch}	open channel friction factor (= $8gR_hS/V^2$)
f_{CW}	friction factor computed using Colebrook-White formula
f_E	equivalent friction factor(= $m_f f_{ch}$)
h	flow depth
k	constant
m	constant
m_f	modification coefficient
m_{Re}	modification coefficient
P	wetted perimeter
Re	Reynolds number for pipe flows (= VD/ν)
Re_E	equivalent Reynolds number (= $m_{Re}Re_{ch}$)
Re_{ch}	Reynolds number for open channel flows (= $4R_hV/\nu$)

R_h	hydraulic radius
S	energy slope
T	temperature of water
u_*	local shear velocity
V	cross-sectional average velocity
w	$= B/(2h)$
x	distance measured laterally from sidewall
y	vertical distance measured from channel bed
α	width-to-depth or aspect ratio for open channel flows ($= B/h$)
ν	kinematic viscosity of fluid
κ	von Karman constant

Table 1. Empirical values of c_1 and c_2 in Eq. (2) for smooth rectangular channels.

Investigator	c_1	c_2
Reinus (1961)	2.00	1.06
Tracy and Lester (1961)	2.03	1.30
Myers (1982)	2.10	1.56
Knight (1984)	1.81	0.35
Yen (2002)	2 – 2.14	0.47 – 1.83
Prandtl (pipe flow)	2	0.8

Table 2
Click here to download Table: Table 2.doc

Table 2. Summary of Experimental Data

No.	Discharge (10^{-3} m^3/s)	Width B (m)	Height h (m)	Slope (10^{-3})	Temperature (^oC)	No.	Discharge (10^{-3} m^3/s)	Width B (m)	Height h (m)	Slope (10^{-3})	Temperature (^oC)
1	0.95	0.3	0.020	0.586	26.8	66	2.86	0.3	0.032	1.049	27.4
2	1.20	0.3	0.023	0.586	26.8	67	3.30	0.3	0.035	1.049	27.4
3	1.38	0.3	0.025	0.586	26.8	68	3.55	0.3	0.037	1.049	27.4
4	1.55	0.3	0.027	0.586	26.8	69	3.94	0.3	0.040	1.049	27.4
5	1.77	0.3	0.030	0.586	26.8	70	4.87	0.3	0.045	1.049	27.4
6	2.07	0.3	0.033	0.586	26.8	71	5.72	0.3	0.050	1.049	27.4
7	2.35	0.3	0.035	0.586	26.8	72	6.54	0.3	0.055	1.049	27.4
8	2.55	0.3	0.037	0.586	26.8	73	7.40	0.3	0.060	1.049	27.4
9	2.91	0.3	0.040	0.586	26.8	74	8.23	0.3	0.065	1.049	26.6
10	3.42	0.3	0.045	0.586	26.8	75	9.44	0.3	0.070	1.049	26.6
11	4.09	0.3	0.050	0.586	26.8	76	10.31	0.3	0.075	1.049	26.6
12	5.44	0.3	0.060	0.586	26.8	77	11.30	0.3	0.080	1.049	26.6
13	6.73	0.3	0.070	0.586	26.8	78	12.35	0.3	0.085	1.049	26.6
14	8.23	0.3	0.080	0.586	26.8	79	13.41	0.3	0.090	1.049	26.6
15	9.58	0.3	0.090	0.586	26.8	80	14.48	0.3	0.095	1.049	26.6
16	11.09	0.3	0.100	0.586	26.8	81	15.54	0.3	0.100	1.049	26.6
17	13.05	0.3	0.110	0.586	26.8	82	16.63	0.3	0.105	1.049	26.6
18	14.48	0.3	0.120	0.586	26.8	83	17.76	0.3	0.110	1.049	26.6
19	16.28	0.3	0.130	0.586	26.8	84	19.02	0.3	0.115	1.049	26.6
20	17.70	0.3	0.140	0.586	26.8	85	20.18	0.3	0.120	1.049	26.6
21	19.80	0.3	0.150	0.586	26.8	86	21.26	0.3	0.125	1.049	26.6
22	2.64	0.3	0.030	1.141	26.5	87	22.35	0.3	0.130	1.049	26.6
23	3.10	0.3	0.033	1.141	26.5	88	11.11	0.6	0.055	0.669	28.5
24	3.38	0.3	0.035	1.141	26.5	89	11.94	0.6	0.057	0.669	28.5
25	3.77	0.3	0.037	1.141	26.5	90	13.06	0.6	0.060	0.669	29.2
26	4.24	0.3	0.040	1.141	26.5	91	15.00	0.6	0.066	0.669	29.2
27	5.04	0.3	0.045	1.141	26.5	92	16.94	0.6	0.072	0.669	26.8
28	5.93	0.3	0.050	1.141	26.5	93	19.44	0.6	0.078	0.669	26.8
29	6.86	0.3	0.055	1.141	26.5	94	22.22	0.6	0.085	0.669	26.8
30	7.87	0.3	0.060	1.141	26.5	95	25.14	0.6	0.093	0.669	26.8
31	8.68	0.3	0.065	1.141	26.5	96	27.92	0.6	0.100	0.669	26.8
32	9.64	0.3	0.070	1.141	26.5	97	31.39	0.6	0.108	0.669	26.8
33	10.87	0.3	0.075	1.141	26.5	98	34.44	0.6	0.113	0.669	28.0
34	11.76	0.3	0.080	1.141	26.5	99	36.81	0.6	0.118	0.669	28.0
35	13.02	0.3	0.085	1.141	26.5	100	42.50	0.6	0.131	0.669	28.0
36	14.23	0.3	0.090	1.141	26.5	101	46.25	0.6	0.139	0.669	29.5
37	15.29	0.3	0.095	1.141	26.5	102	49.58	0.6	0.146	0.669	29.5
38	16.26	0.3	0.100	1.141	26.5	103	54.03	0.6	0.153	0.669	29.5
39	17.57	0.3	0.105	1.141	26.5	104	56.67	0.6	0.160	0.669	29.5
40	18.60	0.3	0.110	1.141	26.5	105	61.94	0.6	0.170	0.669	29.5

41	19.73	0.3	0.115	1.141	26.5	106	68.75	0.6	0.183	0.669	29.5
42	21.30	0.3	0.120	1.141	26.8	107	80.28	0.6	0.204	0.669	29.5
43	22.35	0.3	0.126	1.141	26.8	108	95.28	0.6	0.232	0.669	30.8
44	22.11	0.3	0.110	1.484	26.3	109	122.08	0.6	0.277	0.669	30.8
45	20.53	0.3	0.105	1.484	26.0	110	4.08	0.6	0.042	0.242	26.5
46	18.83	0.3	0.100	1.484	26.0	111	5.39	0.6	0.050	0.242	26.5
47	17.54	0.3	0.095	1.484	26.3	112	6.11	0.6	0.054	0.242	26.5
48	16.39	0.3	0.090	1.484	26.3	113	7.36	0.6	0.061	0.242	26.5
49	15.13	0.3	0.085	1.484	26.3	114	8.33	0.6	0.067	0.242	26.4
50	13.89	0.3	0.080	1.484	26.3	115	9.58	0.6	0.072	0.242	26.4
51	13.24	0.3	0.078	1.484	26.3	116	12.22	0.6	0.084	0.242	26.4
52	12.62	0.3	0.075	1.484	26.3	117	14.72	0.6	0.094	0.242	27.0
53	11.97	0.3	0.072	1.484	26.3	118	17.50	0.6	0.107	0.242	27.0
54	11.31	0.3	0.070	1.484	26.3	119	20.00	0.6	0.117	0.242	27.0
55	10.74	0.3	0.067	1.484	26.3	120	22.64	0.6	0.126	0.242	27.0
56	10.15	0.3	0.065	1.484	26.3	121	26.47	0.6	0.140	0.242	27.0
57	9.59	0.3	0.062	1.484	26.3	122	0.19	0.075	0.020	0.6	26.4
58	9.10	0.3	0.060	1.484	26.3	123	0.28	0.075	0.025	0.6	26.4
59	15.71	0.3	0.080	1.89	26.5	124	0.36	0.075	0.030	0.6	26.4
60	17.40	0.3	0.085	1.89	26.5	125	0.46	0.075	0.035	0.6	26.4
61	17.45	0.3	0.086	1.89	26.5	126	0.49	0.075	0.040	0.6	26.4
62	18.78	0.3	0.090	1.89	26.5	127	0.68	0.075	0.050	0.6	26.0
63	20.24	0.3	0.095	1.89	26.5	128	0.80	0.075	0.055	0.6	26.0
64	22.17	0.3	0.100	1.89	26.5	129	0.90	0.075	0.060	0.6	26.0
65	2.53	0.3	0.030	1.049	27.4	130	1.04	0.075	0.070	0.6	25.4

Table 3 (new)

Table 3. Range of data used for comparisons

Investigator	Re		f		α	
	max	min	max	min	max	min
Tracy and Lester (1961)	726900	35720	0.0257	0.0128	40.37	6.96
Knight (1984)	164087	27051	0.0267	0.0178	19.12	0.31
This study	539700	7657	0.0384	0.0140	15.00	1.07

Table 4. Summary of errors in channel friction predictions

Approach	m_{Re}	m_f	B > 2h		B ≤ 2h	
			Average error (%)	Maximum error (%)	Average error (%)	Maximum error (%)
Jones (1976)	Eq. (8)	1	7.7	19.7	10.9	19.7
Kazemipour and Apelt (1979)	1	Eq. (4)	2.8	16.3	7.4	16.3
Obot(1988)	Eq. (10)	1	7.7	19.2	9.9	17.2
Pillai (1997)	1	Eq. (5)	2.8	16.1	5.7	13.0
Prandtl's friction law	1	1	9.1	20.4	10.2	17.5
Present study Eq. (20)	Eq. (22)	Eq. (21)	2.1	17.4	3.4	10.5
Present study Eq. (23)	-	-	2.1	17.1	3.5	10.9

Figure 1

Click here to download Figure: Fig. 1. Comparison of channel resistance data with Prandtl friction law..pdf

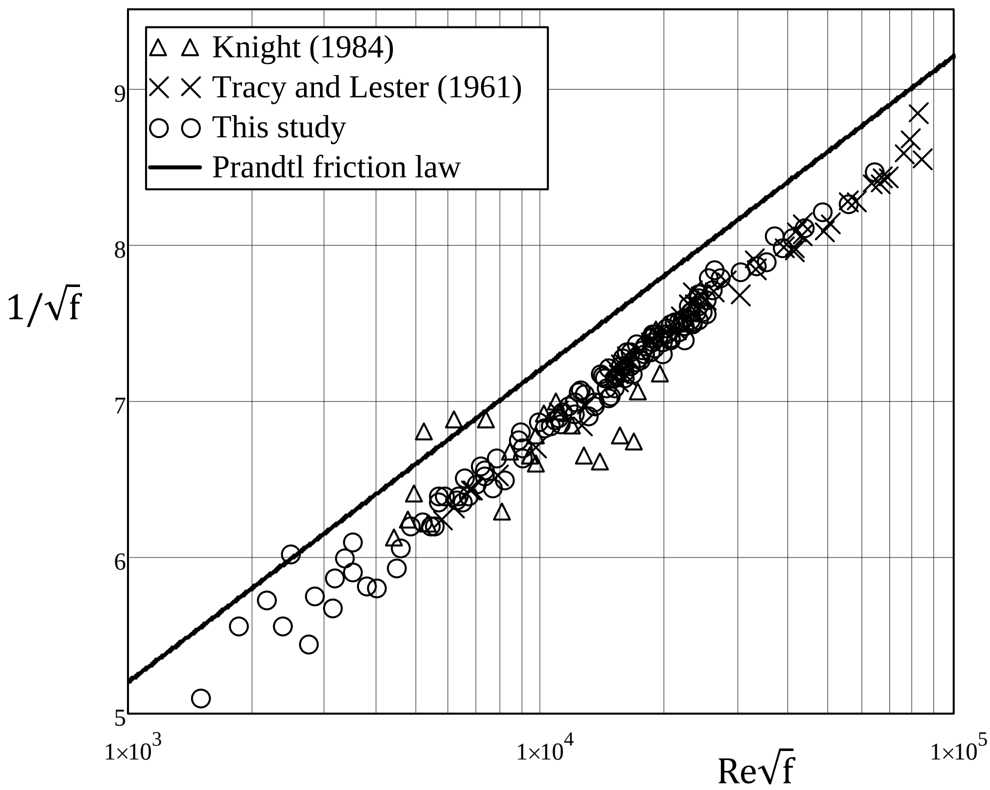

Fig. 1. Comparison of channel resistance data with Prandtl friction law.

Figure 2
Click here to download Figure: Fig. 2. Aspect-ratio effect on the parameter.pdf

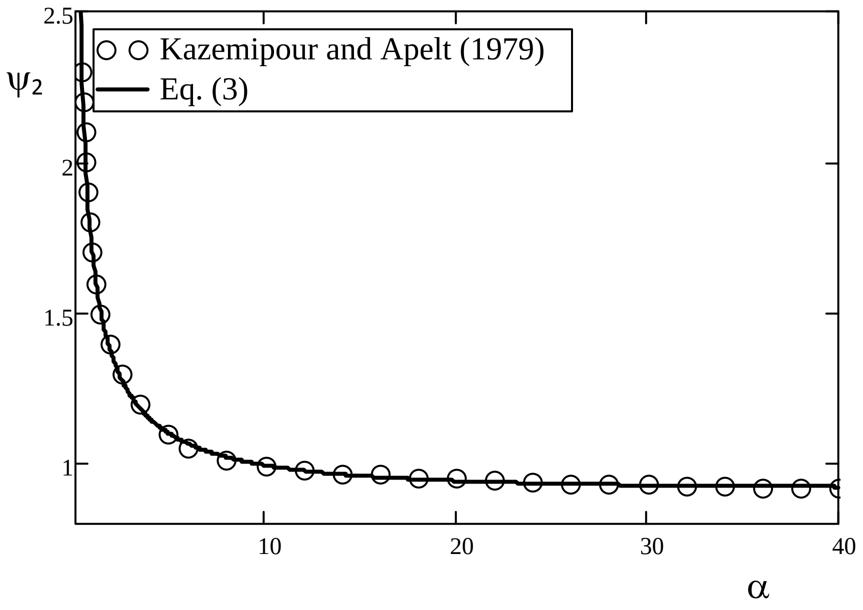

Fig. 2. Aspect-ratio effect on the parameter, ψ_2, proposed by Kazemipour and Apelt (1979).

The circles are the points read from Kazemipour and Apelt's curve.

Figure 3

Click here to download Figure: Fig. 3. Comparison of mf given by Kazemipour and Apelt (1979) and Pillai.pdf

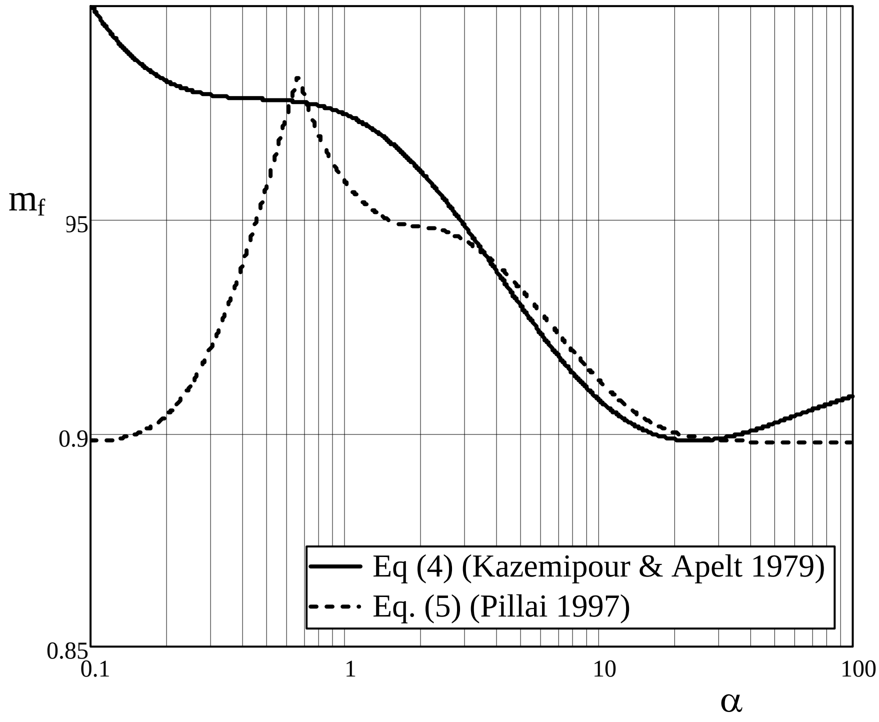

Fig. 3. Comparison of m_f given by Kazemipour and Apelt (1979) and Pillai (1997), respectively.

Figure 4

Click here to download Figure: Fig. 4. Relations of mRe to aspect ratio for rectangular ducts, proposed by Jones (1976) and

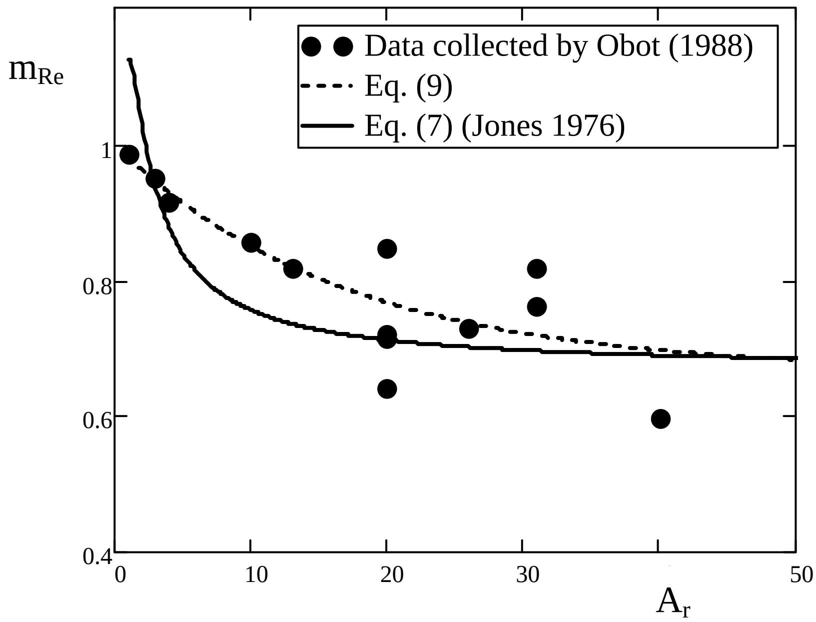

Fig. 4. Relations of m_{Re} to aspect ratio for rectangular ducts, proposed by Jones (1976) and Obot (1988), respectively.

Figure 5
Click here to download Figure: Fig. 5. Division of rectangular cross section.pdf

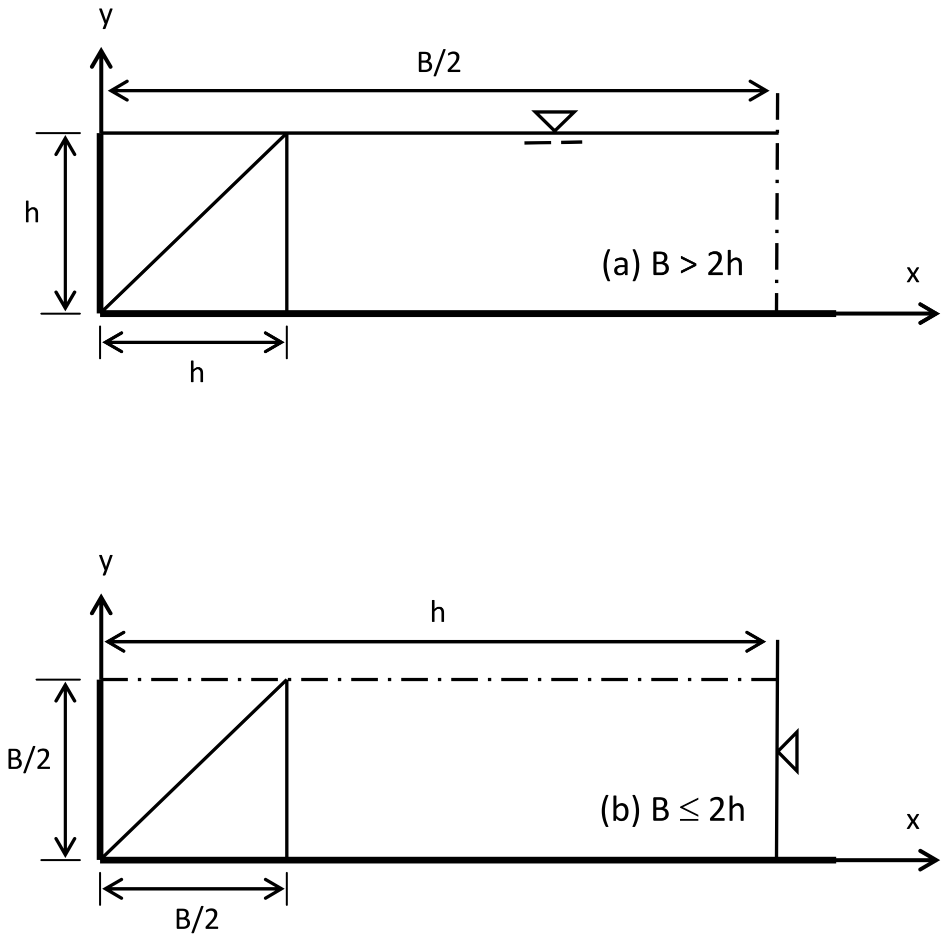

Fig. 5. Division of rectangular cross section for (a) B > 2h and (b) B ≤ 2h.

Figure 6

Click here to download Figure: Fig. 6. Bed shear stress distribution in smooth rectangular channels. Data were collected by

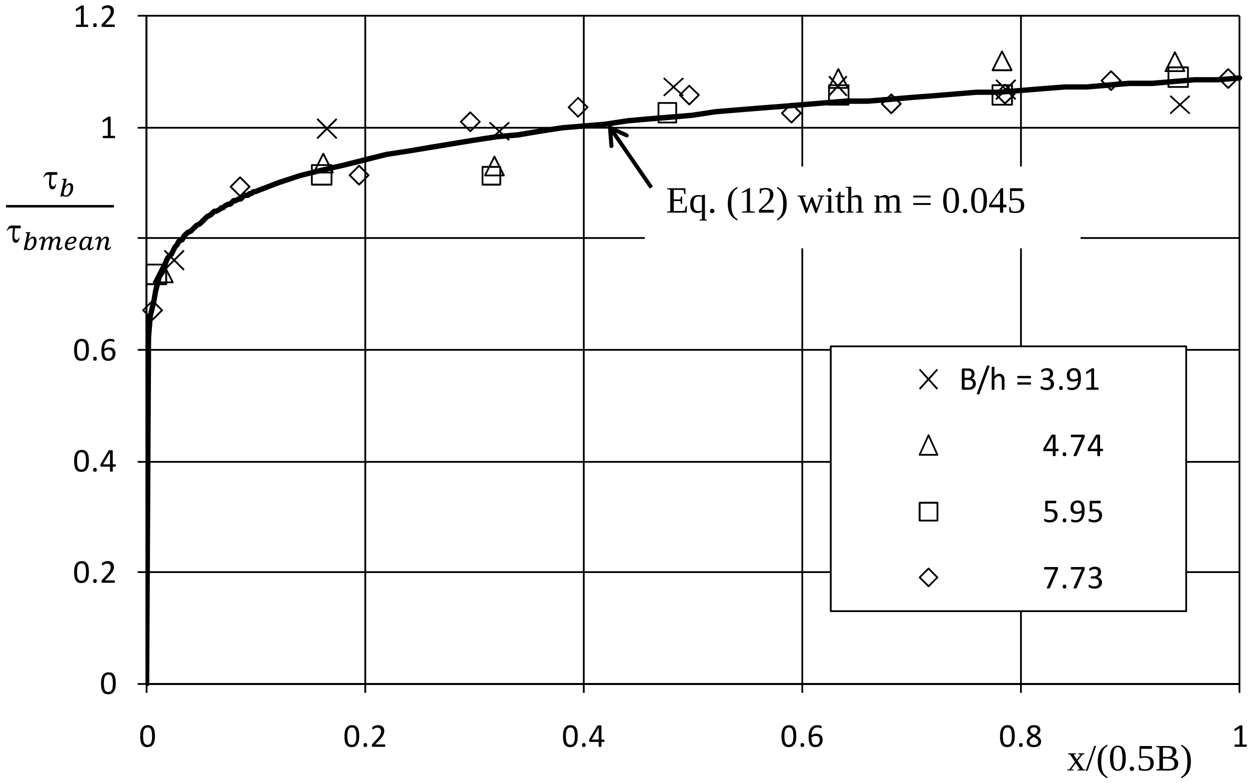

Fig. 6. Bed shear stress distribution in smooth rectangular channels. Data were collected by Knight (1984).

Figure 7
Click here to download Figure: Fig. 7. Variations of prediction error.pdf

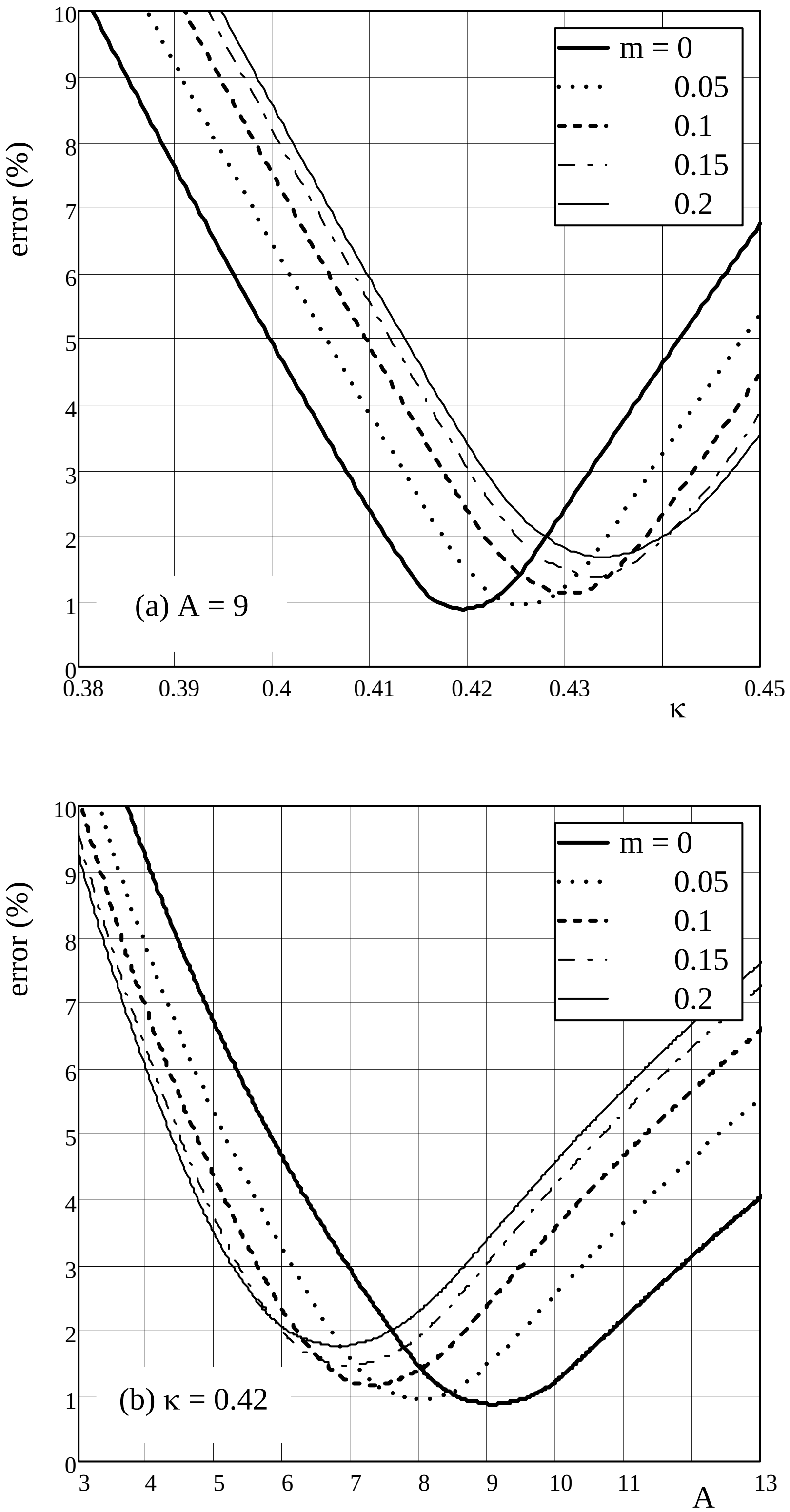

Fig. 7. Variations of prediction error (a) with m and κ for the case of A = 9, and (b) with m and A for the case of κ = 0.42.

Figure 8
Click here to download Figure: Fig. 8. Ranges of prediction error varying with.pdf

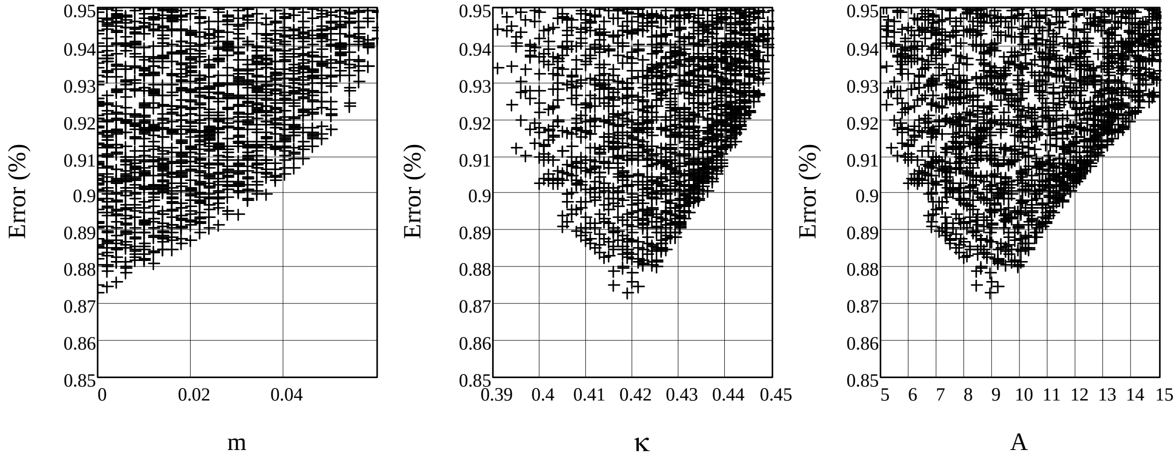

Fig. 8. Ranges of prediction error varying with m, κ and A. The data used are from Tracy and Lester (1961).

Figure 9 (revised)
Click here to download Figure: Fig. 9. Comparison of different approaches (revised).pdf

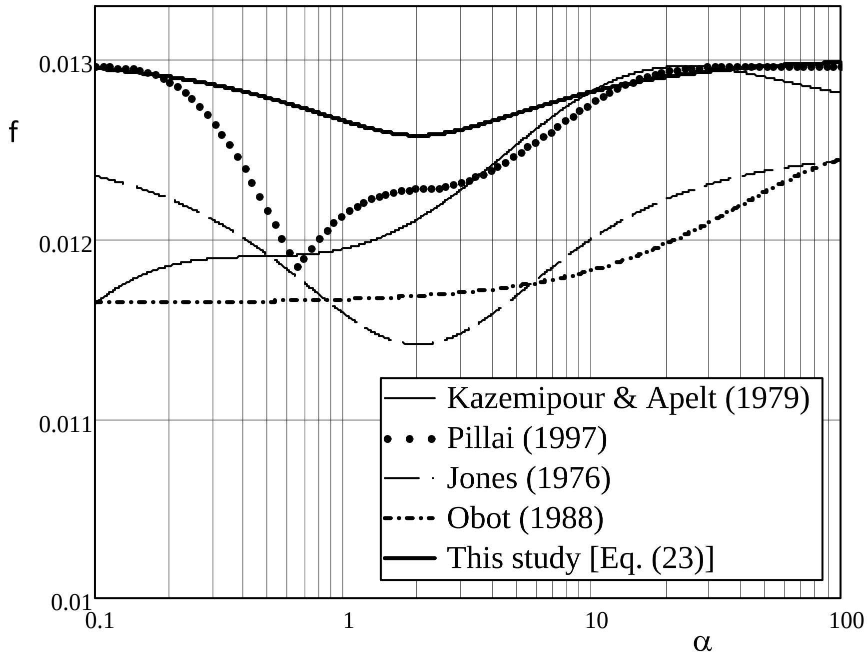

Fig. 9. Comparison of different approaches for predicting friction factor at Re = 10^6.

Figure 10 (revised)

Click here to download Figure: Fig. 10. Comparisons of measured and predicted friction factors (revised).pdf

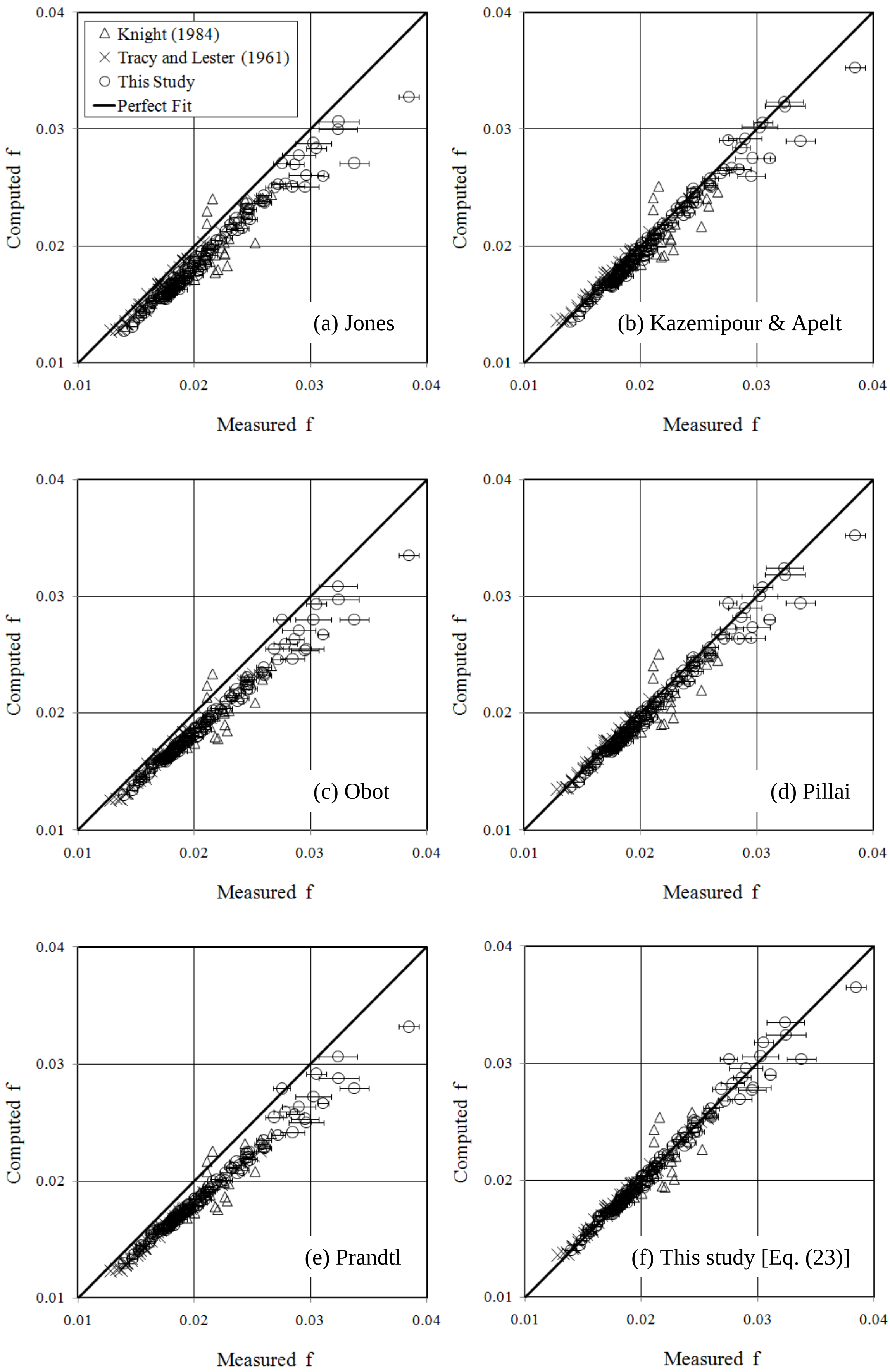

Fig. 10. Comparisons of measured and predicted friction factors

Figure 11 (new)

Click here to download Figure: Fig. 11. Error distribution related to friction factor prediction with Eq. (23)..pdf

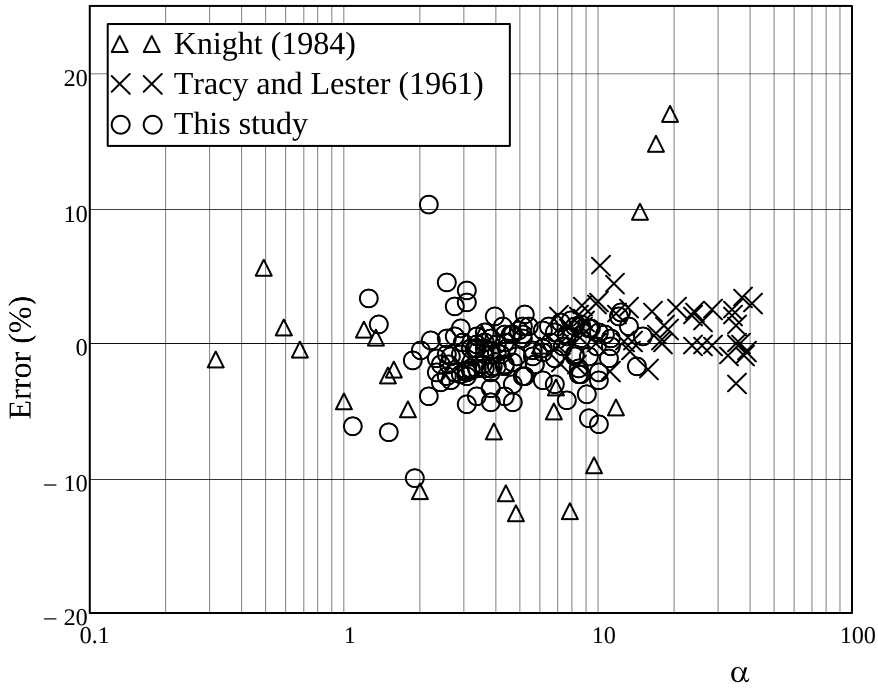

Fig. 11. Distribution of errors in friction factor prediction with Eq. (23).

List of Figure Captions

Fig. 1. Comparison of channel resistance data with Prandtl friction law.

Fig. 2. Aspect-ratio effect on the parameter, ψ_2, proposed by Kazemipour and Apelt (1979). The circles are the points read from Kazemipour and Apelt's curve.

Fig. 3. Comparison of m_f given by Kazemipour and Apelt (1979) and Pillai (1997), respectively.

Fig. 4. Relations of m_{Re} to aspect ratio for rectangular ducts, proposed by Jones (1976) and Obot (1988), respectively.

Fig. 5. Division of rectangular cross section for (a) $B > 2h$ and (b) $B \leq 2h$.

Fig. 6. Bed shear stress distribution in smooth rectangular channels. Data were collected by Knight (1984).

Fig. 7. Variations of prediction error (a) with m and κ for the case of A = 9, and (b) with m and A for the case of $\kappa = 0.42$.

Fig. 8. Ranges of prediction error varying with m, κ and A. The data used are from Tracy and Lester (1961).

Fig. 9. Comparison of different approaches for predicting friction factor at $Re = 10^6$.

Fig. 10. Comparisons of measured and predicted friction factors.

Fig. 11. Distribution of errors in friction factor prediction with Eq. (23).